

Multi- and hyperspectral classification of soft-bottom intertidal vegetation using a spectral library for coastal biodiversity remote sensing

Bede Ffinian Rowe Davies ^{a,*}, Pierre Gernez ^a, Andréa Geraud ^a, Simon Oiry ^a, Philippe Rosa ^a, Maria Laura Zoffoli ^b, Laurent Barillé ^a

^a Nantes Université, Institut des Substances et Organismes de la Mer, ISOMer, UR2160, Nantes F-44000, France

^b Consiglio Nazionale delle Ricerche, Istituto di Scienze Marine (CNR-ISMAR), Rome, Italy

ARTICLE INFO

Keywords:

Remote sensing
Seagrass mapping
Intertidal mapping
Spectral-radiometry
Satellite spectral data
Machine learning
Essential biodiversity variables
Earth observation

ABSTRACT

Monitoring biodiversity and how anthropogenic pressures impact this is critical, especially as anthropogenically driven climate change continues to affect all ecosystems. Intertidal areas are exposed to particularly high levels of pressures owing to increased population density in coastal areas. Traditional methods of monitoring intertidal areas do not provide datasets with full coverage in a cost-effective or timely manner, and so the use of remote sensing to monitor these areas is becoming more common. Monitoring of ecologically important monospecific habitats, such as seagrass beds, using remote sensing techniques is well documented. However, the ability for multispectral data to distinguish efficiently and accurately between classes of vegetation with similar pigment composition, such as seagrass and green algae, has proved difficult, often requiring hyperspectral data. A machine learning approach was used to differentiate between soft-bottom intertidal vegetation classes when exposed at low tide, comparing 6 different multi- and hyperspectral remote and *in situ* sensors. For the library of 366 spectra, collected across Northern Europe, high accuracy (>80%) was found across all spectral resolutions. While a higher spectral resolution resulted in higher accuracy, there was no discernible increase in accuracy above 10 spectral bands (95%: Sentinel-2 MSI sensor with a spatial resolution of 20 m). This work highlights the ability of multispectral sensors to discriminate intertidal vegetation types, while also showing the most important wavelengths for this discrimination (~530 and ~730 nm), giving recommendations for spectral ranges of future satellite missions. The ability for multispectral sensors to aid in accurate and rapid intertidal vegetation classification at the taxonomic resolution of classes, could be a significant contribution for future sustainable and effective ecosystem management.

1. Introduction

Soft-bottom intertidal ecosystems support a diversity of habitats (seagrass meadows, honeycomb worm reefs, oyster reefs, mudflats) and biological communities worldwide (Mouritsen and Poulin, 2002; Murray et al., 2019; Van Der Maarel, 2003). The richness and diversity these habitats contain help to provide numerous ecosystem services, such as protection against coastal erosion, carbon regulation, oxygen production, seasonal habitat for migratory birds (Zoffoli et al., 2022), and reserves and nurseries for fisheries (Gardner and Finlayson, 2018). However, the significant roles of intertidal areas for biodiversity and the ecosystem services they provide are not universally known (Reddin et al., 2022; Unsworth et al., 2022; Unsworth et al., 2019a, 2019b). Like the majority of coastal ecosystems worldwide, intertidal areas are

exposed and vulnerable to anthropogenic pressures, particularly more so due to their closer proximity to potentially destructive human activity (Green et al., 2021; Murray et al., 2019). Global warming, sea-level rise and the rising frequency of extreme climatic events lead to a reduction of their surface (Masson-Delmotte et al., 2021), and to a diminution of their capability to recover from perturbations (Schiel et al., 2021). The effects of climate change impact intertidal habitats inconsistently; declines of certain species and the proliferation of others (Bryndum-Buchholz et al., 2019). Intertidal areas are also directly degraded by human activities, such as coastal urbanization (Momota and Hosokawa, 2021), use of various biochemical contaminants (Durou et al., 2007; Hope et al., 2021), eutrophication (Cardoso et al., 2004), land reclamation (Sedano et al., 2021), and shellfish farming (Garmendia et al., 2021). These pressures impact intertidal biodiversity (Beltrand et al., 2022) and the

* Corresponding author.

E-mail addresses: bede.davies@univ-nantes.fr, bedeffinian@gmail.com (B.F.R. Davies).

ecosystem services it provides (Brondízio et al., 2019; Gardner and Finlayson, 2018).

To reduce these impacts and improve the protection of intertidal areas, several measures have been implemented over the past decades in Europe, such as the Water Framework Directive (WFD, Parliament and Council, 2001), and the Marine Strategy Framework Directive (MSFD, Parliament and Council E, 2008). However, according to the Intergovernmental Science-Policy Platform on Biodiversity and Ecosystem Services (IPBES, Brondízio et al., 2019), current efforts are insufficient to reach the objectives of ecosystem conservation and sustainable exploitation. The ecological status of many intertidal areas have never been evaluated, with many areas uncharacterised. Even in documented areas, there are many socio-environmental challenges to implementing efficient protection and sustainable exploitation (Unsworth et al., 2019a). Providing updated and accurate maps of intertidal areas is a prerequisite to addressing such challenges (McKenzie et al., 2020). However, the traditional methods for mapping rely on field surveys to estimate species abundance, biomass and habitat surface, which are time-consuming and labor-intensive (Nijland et al., 2019; Olmedo-Masat et al., 2020). The collected data are also limited by sampling constraints, as many intertidal areas are difficult to access. Remote sensing can overcome these issues by acquiring temporally and spatially resolved observations of coastal areas (Papathanasiou et al., 2019; Veettil et al., 2020). Likewise, the use of drones can increase the surveyed area compared to traditional survey methods while providing greater spatial resolution and flexibility than satellite imagery (Gomes et al., 2018).

Marine vegetation, defined as any species of plant that, at any time in its life, must inhabit water, other than freshwater, includes a wide range of highly important intertidal species, such as seagrasses, mangroves and marine algae. In the visible and near-infrared range (VNIR), exposed intertidal vegetation can be identified by its spectral reflectance (Douay et al., 2022; Olmedo-Masat et al., 2020). Solar irradiance is absorbed by plant pigments in the visible spectral range (400 to 700 nm: Hallik et al., 2017), while in the NIR range (700 to 900 nm), light is reflected by tissues in pluricellular organisms (Ustin and Jacquemoud, 2020), and by the sediment background for biofilms composed of unicellular photoautotrophs (Barillé et al., 2011). The spectral signature or lack thereof can be used as a marker of the different classes of organisms (Thorhaug et al., 2007). Reflectance is increasingly being used to measure Essential Biodiversity Variables (EBVs) in coastal ecosystems, such as species traits or ecosystem structure and function (Muller-Karger et al., 2018; Pereira et al., 2013). Time-series derived from satellite observations also make it possible to study changes in biodiversity metrics and environmental drivers over decades, as demonstrated recently for the monitoring of seagrass status (Lizcano-Sandoval et al., 2022; Zoffoli et al., 2021), or macroalgae invasions (Hu et al., 2017; Santos et al., 2020). Most satellite sensors are multispectral (Joyce et al., 2009; Xue and Su, 2017), and generally measure the reflectance using three to ten spectral bands in the VNIR spectral domain. Depending on the band numbers and characteristics, the discrimination of different types of marine vegetation can be limited (Casal et al., 2013; Kutser et al., 2006). Hyperspectral missions such as PRRecursore IperSpettrale della Missione Applicativa (PRISMA), or EnMAP acquiring data along a large number of narrow spectral bands could improve habitat identification accuracy (Hestir et al., 2015; Ustin et al., 2004). However, these sensors often provide relatively low spatial and temporal resolutions (Veettil et al., 2020), can contain high levels of noise per spectral band, and are not openly available resources (e.g. PRISMA imagery: 30 m pixel size, 29 day orbit repeat cycle and are only available on prior request or EnMAP imagery: 30 m pixel size and a 27 day orbit repeat cycle).

Mapping intertidal habitats of ecological importance, such as seagrass beds, can be achieved with a multispectral resolution in the case of exposed monospecific meadows observed during low tide (Zoffoli et al., 2020, 2022). However, when seagrass are mixed with other green vegetation, discrimination with multi- or even hyperspectral sensors (*in situ* and satellite) is challenging (Phinn et al., 2018; Veettil et al., 2020).

Green macroalgae and more specifically the taxonomic class of Ulvophyceae share the same pigmentary composition with seagrass and should be *a priori* more complex to discriminate (Oiry and Barillé, 2021). Other taxonomic classes common in intertidal soft-bottom environments such as Xanthophyceae and Bacillariophyceae could also be confused with seagrass when present at low cover (Zoffoli et al., 2020). It is generally agreed that the identification at broad taxonomic levels (e.g. class level) is more precise than at the species level (Casal et al., 2013; Kutser et al., 2006). Assessing the ability of a sensor to discriminate seagrass meadows from other intertidal vegetation can be explored with spectral libraries. They have been used to study the spectral discrimination between macroalgal species (Casal et al., 2013; Chao Rodríguez et al., 2017; Dierssen et al., 2015; Douay et al., 2022; McIlwaine et al., 2019; Olmedo-Masat et al., 2020), and to identify different seagrass species (Fyfe, 2003) or to differentiate seagrass from other nearshore vegetation types (Légaré et al., 2022). By applying to *in situ* spectra collected with a spectroradiometer the spectral responses function of multi- and hyperspectral sensors, it is possible to investigate their abilities to classify intertidal green macrophytes. In particular, the possibility to discriminate seagrass from green macroalgae at a multispectral resolution remains to be studied using machine learning approaches.

This study aimed at analysing the potential of multi- and hyperspectral satellite missions (Pleiades, Sentinel-2, and PRISMA), as well as a multispectral drone sensor, for the discrimination of green macrophytes from low tide soft-bottom intertidal areas when exposed using remote sensing. A spectral library of the spectral signatures of seagrass, green macroalgae, and other intertidal vegetation was compiled from measurements performed with a field spectroradiometer. This library represents a novel taxonomic and spatial coverage with spectra from a wide array of exposed soft-bottom intertidal habitats collected across almost 15 degrees of latitude. High-resolution spectra were degraded to each sensor spectral resolution. A combination of multivariate and machine learning algorithms were then performed to compare the ability of the different spectral resolution data at distinguishing the main taxonomic classes of intertidal vegetation. The wavelengths which best discriminated green macrophytes were identified and recommendations given on potential future satellite sensors.

2. Materials and methods

2.1. Spectral reflectance acquisition

Spectral reflectance data were collected from a range of macroalgal, microphytobenthic and seagrass dominated soft-bottom intertidal areas. Samples were grouped at the class level: Magnoliopsida (Seagrasses), Ulvophyceae (Green Macroalgae), Phaeophyceae (Brown Macroalgae), Xanthophyceae (Yellow Algae) and Bacillariophyceae (Diatoms: Table 1 & Fig. 1). Brown macroalgae growing on rocky substrates were added as they are often found stranded in the intertidal zone. Spectral reflectance were also recorded from sediment areas without clear vegetation, hereafter referred to as “bare sediment” for the sake of simplicity. Scientific names and taxonomy were based on the World Register of Marine Species (WORMS). Species were identified *in situ* when recently exposed but not covered by a layer of water.

Multiple field campaigns taking place from 2 h prior to 2 h post minimum tide were carried out across temperate intertidal areas along the Western Atlantic coastline during the summer months (Fig. 2). The campaigns took place in France in Bourgneuf Bay (Barillé et al., 2010, 2011; Zoffoli et al., 2020), Marennes-Oléron Bay, Auray Estuary, Mont-Saint-Michel Bay, Morbihan Gulf and Traict of Merquel, in Spain in Bolonia Beach (Roca et al., 2022) and Bay of Cadiz (Zoffoli et al., 2020), and in Portugal in the Tagus Estuary and Aveiro Lagoon.

Most spectral data were collected with an ASD FieldSpec HandHeld 2 spectroradiometer (Roca et al., 2022; e.g.: Zoffoli et al., 2020), which was wavelength calibrated using a mercury-argon low pressure lamp. The spectral library of Bacillariophyceae had been obtained with a

Table 1

Number of spectra samples taken across species and classes with references of where and when the data were collected. Mont Saint-Michel Bay was abbreviated to MSM. The location of sampling sites are shown in Fig. 2.

Class	Species	Number of Spectra	Site	Reference
Magnoliopsida				
Ulvophyceae	<i>Zostera noltei</i>	58	Bourgneuf Bay, Marennes-Oléron Bay, Cadiz Bay, Tagus Estuary, Aveiro Lagoon and Traict of Merquel	Zoffoli et al., 2020 and this study
	<i>Zostera marina</i>	23	Bourgneuf Bay	This study
Xanthophyceae				
Phaeophyceae	<i>Ulva sp.</i>	16	Bourgneuf Bay, Auray Estuary, MSM, Tagus Estuary, Aveiro Lagoon and Traict of Merquel	Barillé et al., 2010 and this study
	<i>Ulva ramosa</i>	3	Bourgneuf Bay	This study
Bacillariophyceae	<i>Ulva linza</i>	33	Traict of Merquel	This study
	<i>Chaetomorpha sp.</i>	21	Morbihan Gulf	This study
	<i>Cladophora sp.</i>	11	Morbihan Gulf	This study
	<i>Ulva lactuca</i>	34	Morbihan Gulf	This study
	<i>Codium fragile</i>	3	Morbihan Gulf	This study
	<i>Vaucheria sp.</i>	33	Bourgneuf Bay	This study
Fucus vesiculosus				
Bacillariophyceae	<i>Fucus vesiculosus</i>	27	MSM, Bourgneuf Bay, Morbihan Gulf, Tagus Estuary and Aveiro Lagoon	This study
	<i>Fucus serratus</i>	6	MSM	This study
	<i>Fucus spiralis</i>	13	Morbihan Gulf	This study
	<i>Ascophyllum nodosum</i>	13	MSM, Auray Estuary, Morbihan Gulf	This study
	<i>Rugulopteryx okamurae</i>	5	Bolonia Beach	Roca et al., 2022
<i>Navicula ramosissima</i>				
<i>Entonomeis paludosa</i>	<i>Navicula ramosissima</i>	10	Bourgneuf Bay	Barillé et al., 2011
	<i>Gyrosigma limosum</i>	21	Bourgneuf Bay	Barillé et al., 2011
	<i>Gyrosigma limosum</i>	2	Bourgneuf Bay	Barillé et al., 2011

GER3700 spectroradiometer (Barillé et al., 2011). Reflectance was measured in the visible near-infrared (VNIR) either from 325 to 1075 nm with the ASD spectroradiometer, or from 350 to 1050 nm with the GER3700 spectroradiometer (Barillé et al., 2010). Both instruments were used without glass fiber probe and had a spectral resolution of 3 ± 1 nm, at the Full Width Half Maximum (FWHM), but a slightly different sampling interval with 1 nm and 1.5 nm for the ASD and GER respectively. ASD spectra were resampled to match the GER resolution. Prior to measurement, internal optimisation was carried out to adjust integration time of the instrument's detectors to the ambient light. After a dark noise calibration, measurements were obtained in reflectance after collecting downwelling radiance over a 99% Spectralon white reference. To reduce instrumental noise during the data acquisition, each sample was measured at least 10 times over ~ 30 s from directly above, with the operator angled at 90° to incoming direct sunlight. The distance of

acquisition was between 30 and 50 cm. As the field of view was $\sim 3.5^\circ$, the measured area varied from 11 to 29 cm^2 . Whatever the size of the measured area, all reflectance measurements were performed on homogeneous vegetation patches, displaying 100% cover (or above bare sediment).

2.2. Data analysis

2.2.1. Spectral degradation

The efficacy, efficiency and ability of classifying intertidal soft-bottom vegetation were assessed for a variety of remote-sensing sensors, including two multispectral satellite sensors (the high-resolution imager (HiRI) onboard Pleiades and the multi-spectral instrument (MSI) onboard Sentinel-2), one hyperspectral satellite sensor (the hyperspectral camera (HYC) onboard PRISMA satellite) and one airborne multispectral sensor (MicaSense RedEdge MX-dual Sensor on board a DJI Matrice 200 drone). These sensors cover a gradient of spectral resolution from multispectral to hyperspectral (Fig. 3). The spectral response functions of Pleiades and Sentinel-2 were used to degrade the hyperspectral library to the respective resolution of each sensors. The highest spatial resolution of Sentinel-2 (10 m) consists of 4 spectral bands while the 20 m sensor has 4 additional bands in the VNIR spectral range (total 8 bands). Sentinel-2 spectral bands, such as at 443 nm, were not used because its spatial resolution (60 m) is too coarse for intertidal seagrass mapping (Zoffoli et al., 2020). To degrade the ASD library to the PRISMA spectral resolution, only central wavelengths and bandwidths (from 400 to 900 nm) were obtained from the Agenzia Spaziale Italiana (ASI, 2020). Likewise, central wavelengths with bandwidths were available for the Micasense ("Drone" henceforth). Therefore, the mean of the reflectance values included in the bandwidth of each PRISMA and Drone function band were computed. Across all sensors, a moving average was applied to the ASD spectral library with a 5 nm smoothing window to reduce instrument-induced noise in the data.

2.2.2. Standardisation

All spectra were standardised to reduce the effect of variable biomass, density or thickness of sample, with a Min-Max transformation (Cao et al., 2017). This calculation emphasised the spectral shapes in the visible range associated with the pigment composition (Douay et al., 2022):

$$R_i^*(\lambda) = \frac{R_i(\lambda) - \min(R_i)}{\max(R_i) - \min(R_i)}$$

where $R_i(\lambda)$ is the reflectance at a specific wavelength (λ) for a specific spectrum (i), where $\min(R_i)$ and $\max(R_i)$ are the corresponding minimum and maximum values.

2.2.3. Statistical analysis

To visually assess the differences between classes across different spectral resolutions dissimilarity matrices were computed for all vegetative classes, with the cosine distance to compute a Spectral Angle Mapper (SAM). The SAM algorithm considers that each spectrum is a vector in n -dimensions space, n being the number of bands, and measures the angle between two spectra to determine their dissimilarity (Kruse et al., 1993). The difference between classes were visualised and statistically assessed with non-metric Multi-Dimensional Scaling (nMDS) ordination and Analysis of Similarity (ANOSIM) from the 'vegan' package within the programming language R (Oksanen et al., 2022). ANOSIM was carried out on the SAM distance matrix using 999 permutations.

To assess the ability of different sensors at classifying intertidal vegetative and non vegetative classes (bare sediments, Bacillariophyceae, Magnoliopsida, Phaeophyceae, Ulvophyceae & Xanthophyceae) from their spectral reflectance data, supervised Machine Learning (ML) algorithms were applied from the "tidymodels" ecosystem of

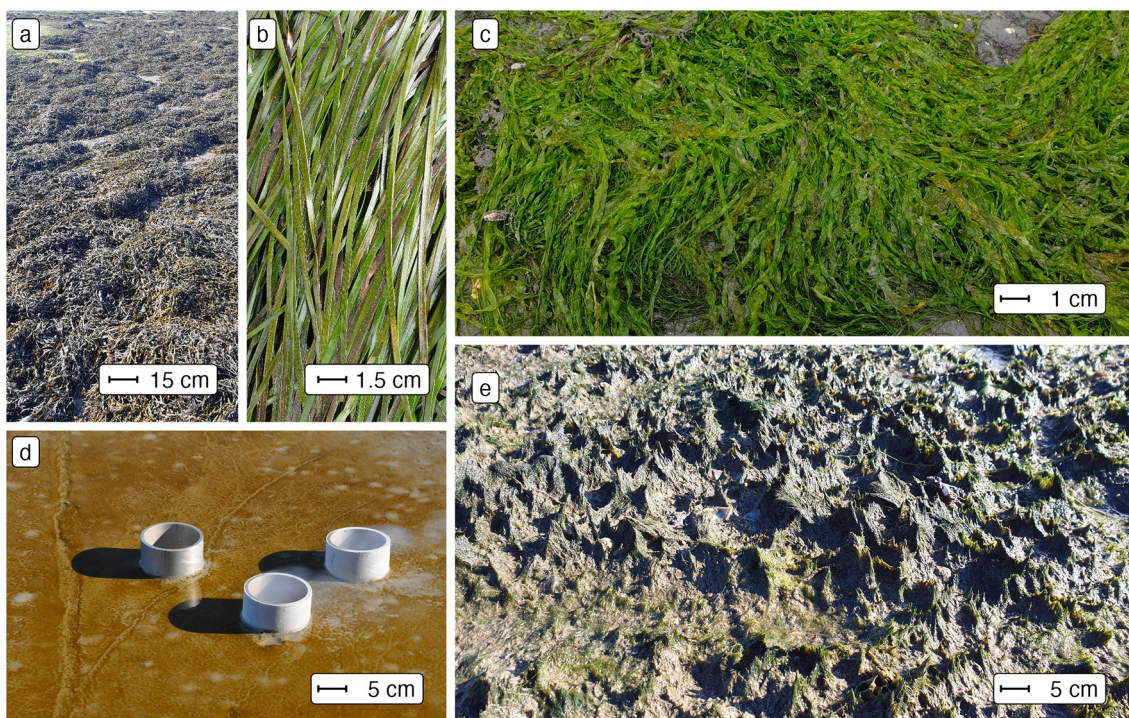


Fig. 1. Examples of taxonomic classes of soft-bottom intertidal vegetation in the field (a: Phaeophyceae (*Fucus vesiculosus*), b: Magnoliopsida (*Zostera noltei*), c: Ulvophyceae (*Ulva linza*), d: Bacillariophyceae (Diatoms) and e: Xanthophyceae (*Vaucheria spp.*)). Scale bars show approximate scale.

packages within the programming language R (Kuhn and Wickham, 2020; R Core Team, 2022). Multiple models were developed (Random Forest, XGBoost and Multinomial Classifiers) with relatively similar results. The model described here was an ensemble decision tree classification approach; Random Forest from the “ranger” package (Wright et al., 2022). As Random Forest employs randomisation of trees, 20 repetitions of the analysis were carried out to avoid over or under representation of specific samples. Spectral data were split into training and testing sets using a proportion of 0.75 to 0.25 using the response variable to stratify samples and reduce group imbalance. Training data were then further split into 30 training and validation datasets using bootstrap resamples to allow hyper-parameter tuning from the “rsample” package (Silge et al., 2022). Class was modelled as a function of all available features (standardised reflectance of each wavelength), where all features displaying zero variance across all classes were removed before model tuning as zero variance values would provide no additional information for the models. This meant only the first three bands of Pleiades and Sentinel-2 at 10 m were evaluated as their highest bands in the NIR showed no variance. Models were tuned to maximise the Area Under the Curve of the Receiver Operating Characteristic (ROC), which measures the diagnostic ability of a classifier based on the ratio of false positive and true positive rate. Accuracy, Cohen’s kappa (an accuracy measure that takes into account class size discrepancy), sensitivity and specificity were calculated using the ‘yardstick’ package, while the ‘vip’ package was used to calculate variable importance (Greenwell et al., 2020; Kuhn et al., 2022). Variable importance will show the relative importance of different wavelengths and was calculated by the prediction error, using permuted out-of-bag data and comparing differences to the prediction error of permuted predictor variables.

3. Results

3.1. Spectral signatures at different spectral resolutions

At hyperspectral resolution (ASD, PRISMA), the differences among

vegetative habitats were obvious, with the highest dissimilarities observed from 550 to 650 nm and from 700 to 850 nm (Fig. 4). In particular, the spectral characteristics among the classes were more conspicuous in the green - red spectral range, such as reflectance peaks at 550 nm (Magnoliopsida, Ulvophyceae, Xanthophyceae), 600 nm (Bacillariophyceae), and 650 nm (Xanthophyceae and Bacillariophyceae). The absorption band at 675 nm, present in every class, corresponded to chlorophyll *a* while at 630 nm a smaller absorption band for the Bacillariophyceae and the Xanthophyceae corresponded to chlorophyll *c*. Phaeophyceae was the class showing the lowest reflectance in the visible range. All classes but the Ulvophyceae had a positive slope in the NIR. The degradation to a multispectral resolution made these spectral features harder and or impossible to distinguish. The differences between vegetation classes were more pronounced for the drone and Sentinel-2 20 m sensors (8–10 spectral bands) than for the Pleiades and Sentinel-2 10 m sensors (4 spectral bands).

3.2. Spectral dissimilarity between the taxonomic classes

The nMDS ordinations calculated with a cosine distance showed that all vegetation classes could be distinguished with a hyperspectral sensor (ASD, PRISMA), despite some overlaps between the Magnoliopsida, Ulvophyceae and Xanthophyceae (Fig. 5). Interestingly, similar ordination patterns were also observed for the multispectral sensors with the highest number of bands (i.e., Drone, Sentinel-2 20 m). The greatest dissimilarity between classes was observed for the ASD ($R = 0.638$ & $p = 0.001$). The differences between PRISMA, the Drone and Sentinel-2 at 20 m were very similar (PRISMA: $R = 0.611$ & $p = 0.001$, Drone: $R = 0.588$ & $p = 0.001$ & Sentinel-2 at 20 m), while Pleiades and Sentinel-2 at 10 m were far lower (Pleiades: $R = 0.49$ & $p = 0.001$ & Sentinel-2 at 10 m). Strong overlaps were observed between the classes Magnoliopsida and Ulvophyceae at the low spectral resolution of Pleiades and Sentinel-2 10 m.

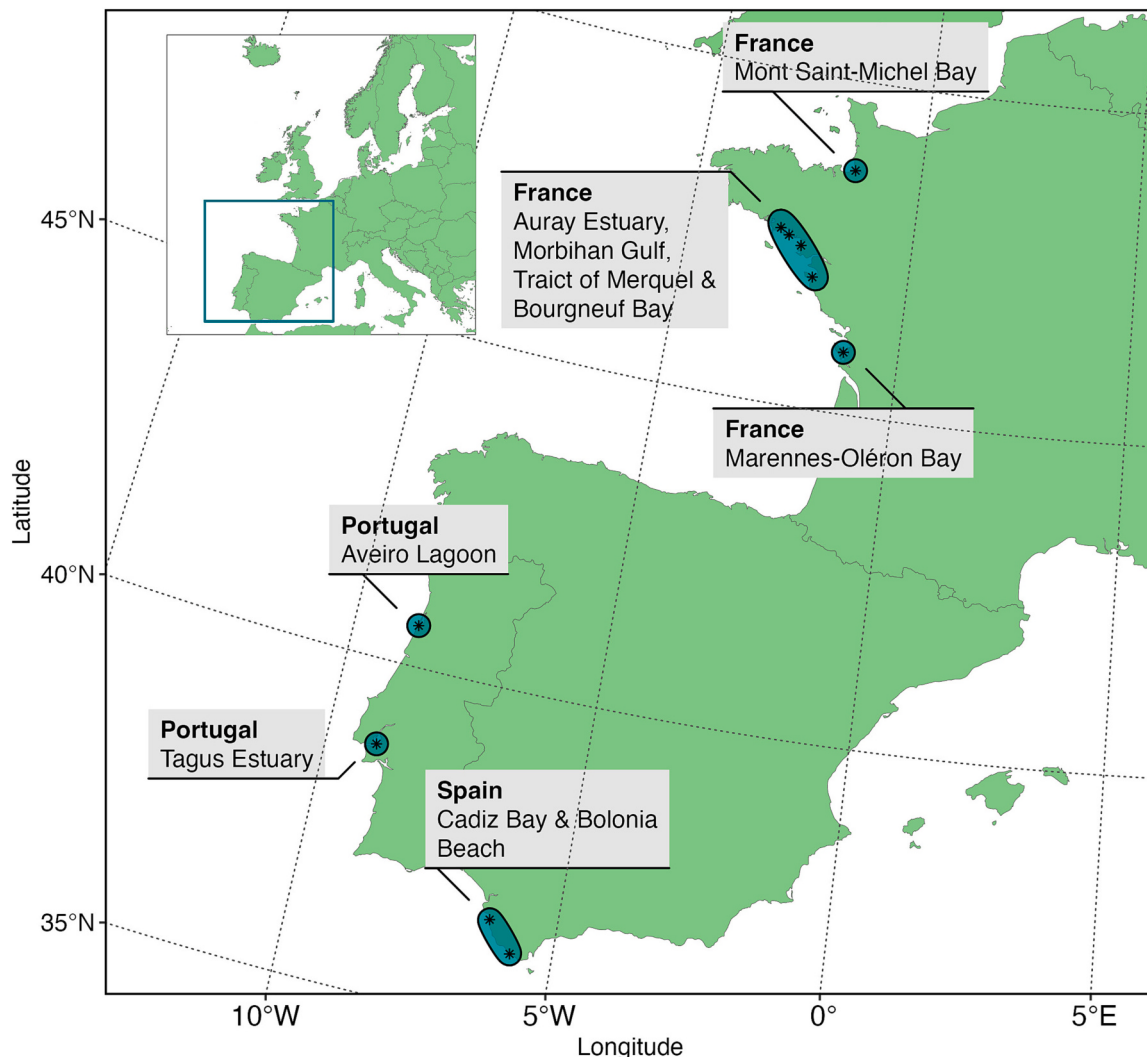


Fig. 2. Sample collection sites across Europe.

3.3. Accuracy across sensors and importance of wavelengths

When assessed by Random Forest modelling, accuracy metrics of different spectral resolutions showed that Sentinel-2 20 m and Drone spectra gave high mean accuracy regardless of accuracy metric (Accuracy: 0.95 ± 0.004 for Sentinel-2 20 m & 0.948 ± 0.004 for Drone. Cohen's Kappa Accuracy: 0.935 ± 0.006 for Sentinel-2 20 m & 0.934 ± 0.005 for Drone: Fig. 6 & Table 2). Above a spectral resolution of 10 bands, there was no gain in mean accuracy even with large increases in spectral resolution (Accuracy: 0.95 ± 0.005 for ASD & 0.951 ± 0.006 for PRISMA. Cohen's Kappa Accuracy: 0.936 ± 0.006 for ASD & 0.938 ± 0.008 for PRISMA). The sensors with the lowest spectral resolution (Pleiades and Sentinel-2 10 m) showed the lowest accuracy, yet still were accurate around 80 to 90% of the time (Accuracy: 0.861 ± 0.006 for Pleiades & 0.835 ± 0.008 for Sentinel-2 10 m. Cohen's Kappa Accuracy: 0.821 ± 0.008 for Pleiades & 0.792 ± 0.005 for Sentinel-2 10 m). Likewise, model specificity and sensitivity showed the greatest values from 8 spectral bands and above, but no increase was shown from 10 to 300 bands (Sensitivity: 0.948 ± 0.006 for Sentinel-2 20 m, 0.941 ± 0.006 for Drone, ± 0.006 for PRISMA & 0.938 ± 0.008 for ASD; Specificity: 0.989 ± 0.001 for Sentinel-2 20 m, 0.989 ± 0.001 for Drone, ± 0.001 for PRISMA & 0.989 ± 0.001 for ASD). Below 8 spectral bands, mean sensitivity and specificity were lowest, yet still around 85% (Sensitivity: 0.847 ± 0.008 for Pleiades & 0.844 ± 0.008 for Sentinel-2

10 m; Specificity: 0.97 ± 0.001 for Pleiades & 0.966 ± 0.002 for Sentinel-2 10 m).

Standardised variable importance, the relative amount the inclusion of a variable in the model affected its' performance, showed the wavelengths the model considered most important (Fig. 7). Consistently across all spectral resolutions, wavelengths 517–556 nm were shown to be highly important. When present, wavelengths around 722–754 nm were the most important.

When the variable importance of the ASD was overlaid on the response functions for the different multispectral sensors, the ability of each sensor to effectively sample the wavelengths of interest become clearer (Fig. 8). The Drone and Pleiades sensors effectively sample the top of the peak in importance from 517 to 556 nm, while Sentinel-2 (10 m and 20 m) is only sampling the edges of the peak. Both Pleiades and Sentinel-2 at 10 m did not sample the highest peak of importance from 722 to 754 nm, while the Drone and Sentinel-2 at 20 m only sampled one side of this peak. Generally, the Drone is sampling all the major and minor peaks of importance apart from one minor peak around 780 nm.

3.4. Confusion matrices

Models accurately classed bare sediments consistently, regardless of spectral resolution (Fig. 9). Ulvophyceae appeared to be mislabeled the most, while Magnoliopsida and Phaeophyceae showed consistently high

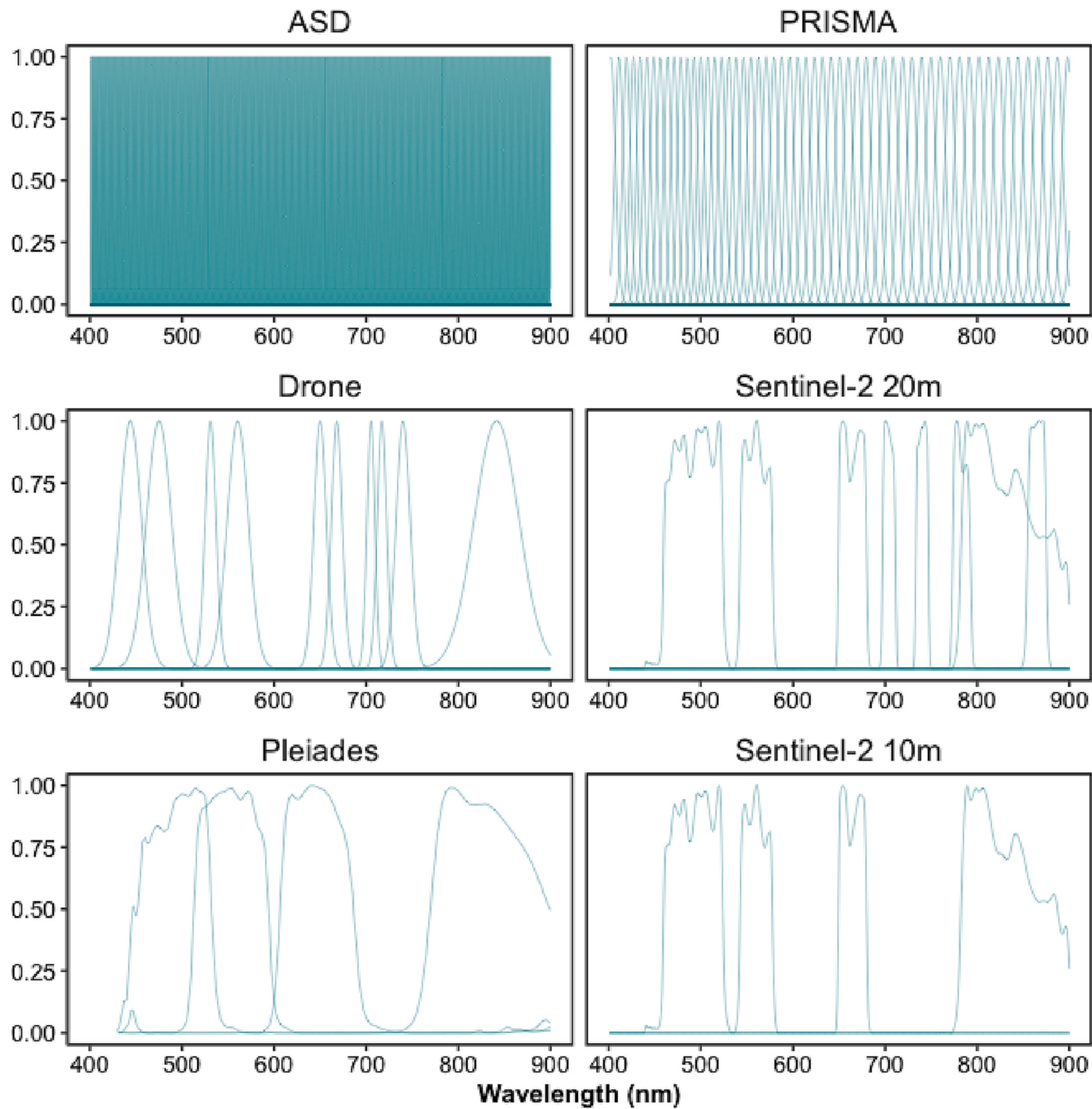


Fig. 3. Spectral response functions for different hyper- and multi-spectral sensors (ASD, Pleiades, Sentinel-2 (10 m), Sentinel-2 (20 m), Drone, and PRISMA).

prediction accuracy, especially by the Drone data. Across all spectral resolutions a small number of Magnoliopsida samples were mislabeled as Bacillariophyceae, Xanthophyceae and Ulvophyceae. A few Bacillariophyceae and Ulvophyceae samples were incorrectly labeled as Magnoliopsida. Likewise, identification of Xanthophyceae was consistently poor across all spectral resolutions apart from Sentinel-2 at 20 m (Sensitivity: 0.79 ASD, 0.87 PRISMA, 0.76 Drone, 0.93 Sentinel-2 at 20 m, 0.7 Sentinel-2 at 10 m and 0.5 Pleiades and Specificity: 0.84 ASD, 0.84 PRISMA, 0.86 Drone, 0.82 Sentinel-2 at 20 m, 0.57 Sentinel-2 at 10 m and 0.53 Pleiades). Pleiades and Sentinel-2 at 10 m had the worst Magnoliopsida classification (Sensitivity: 0.66 Sentinel-2 at 10 m and 0.75 Pleiades; Specificity: 0.79 Sentinel-2 at 10 m and 0.8 Pleiades).

4. Discussion

4.1. Spectral library and vegetation classification

Spectral libraries have been used in coastal areas to analyse the capacity of hyperspectral sensors to discriminate macrophytes at different taxonomic resolutions (Diruit et al., 2022; Douay et al., 2022; McIlwaine et al., 2019; for earlier references see Chao Rodríguez et al., 2017) or to estimate the background contribution on benthic diatoms reflectance spectra (Barillé et al., 2011). The spectral library built up for this work was used to study the discriminatory ability of exposed soft-bottom intertidal vegetation at a class taxonomic level for a variety of remote-sensing instruments. Importantly, the classifier was designed to be

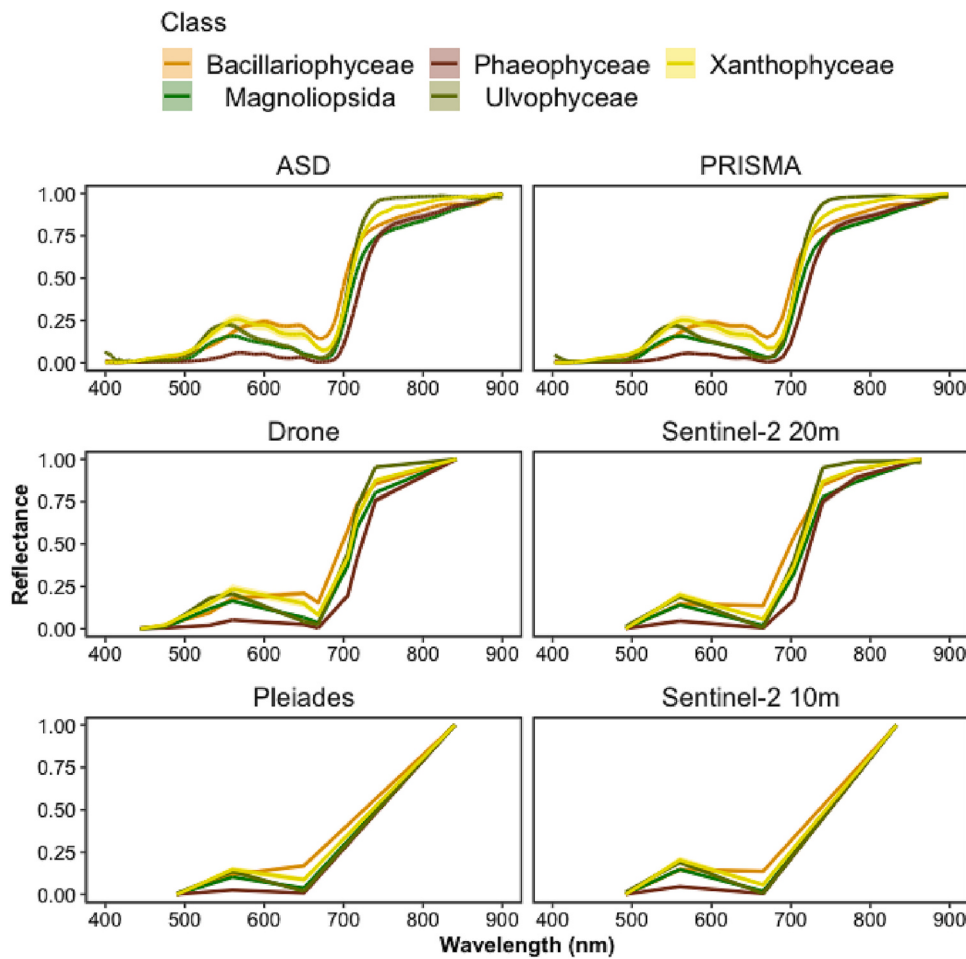


Fig. 4. Spectral signatures of different vegetation classes at different spectral resolutions (ASD, Pleiades, Sentinel-2 10, Sentinel-2 10–20 m, Drone and PRISMA). Lines show mean signature per wavelength, while shading shows 95% confidence interval. Confidence intervals were consistently small and therefore are hard to distinguish.

applicable to both multi- and hyperspectral sensors, which is an advantage compared to classification methods only designed for hyperspectral sensors, such as derivative spectral analysis (Mcilwaine et al., 2019). The discrimination accuracy of the vegetation classes increased with spectral resolution, yet showed diminishing returns for resolutions above ~10 spectral bands. The main result of this study was the capacity to discriminate seagrass from green macroalgae at a multitemporal resolution with ten bands when using machine learning classification techniques. As expected, this discrimination was also possible with hyperspectral sensors. Sensors with a spectral resolution of four bands, such as Pleiades and Sentinel 2 (10 m), were poorer at accurately discriminating between green macroalgae and seagrass, as their spectral shapes were too similar (Fig. 4 & Fig. 6). The importance of effective seagrass classification is considerable, with seagrass conservation and restoration contributing to 16 of the 17 United Nations Sustainable Development Goals (SDGs: Unsworth et al., 2022). A practical restraint of this analysis is the necessity for non-submerged samples. However, the main challenge in mapping seagrass through remote sensing stems from confusion between similarly pigmented green algae, leading to high levels of uncertainty in current seagrass extent (McKenzie et al., 2020). Vegetation classes were consistently distinguishable from bare sediments, as found elsewhere between bare rock and algae (Douay et al., 2022). Likewise, random forest models were successfully able to discriminate between habitats (Légaré et al., 2022; See also: Oiry and Barillé, 2021), with generally lower accuracy at lower spectral resolution, yet even at the lowest spectral resolutions (Pleiades and Sentinel-2 10 m) there was a mean test accuracy of 86.1% and 83.5% respectively

(82.1% and 79.2% respectively when class imbalance was considered with Cohen's kappa).

4.2. Spectral discrimination and pigment composition

Two wavelength regions, respectively in the green (~517–556 nm) and NIR (~722–754 nm) spectral domains, were identified for their importance to the random forest model as contributing most to the discrimination between taxonomic classes (Fig. 7). The wavelength window around 530 nm has already been recommended to distinguish different species of seagrass (Fyfe, 2003), and brown from green macroalgae (Mcilwaine et al., 2019). The spectral differences in the visible range between the classes are partially explained by their difference of pigment composition (Table 3). Pigments have different optical properties and absorption wavelengths, which influence the reflectance spectra shapes. Chlorophyll c and fucoxanthin absorb light at 636 nm and 550 nm respectively (Méléder et al., 2013). Those pigments are present among diatoms and brown macroalgae, but absent in green macrophytes. Xanthophyceae also contain chlorophyll c, but no fucoxanthin (Table 3). Chlorophylls and carotenoids absorptions can thus be used as diagnostic features to identify vegetation types that do not share the same pigmentary composition (Casal et al., 2012; Douay et al., 2022; Méléder et al., 2013). In this work, spectral differences have been observed between two classes having a similar pigment composition, the Magnoliopsida and the Ulvophyceae (Table 3). This indicates that the pigment concentrations and relative proportions, which can vary inside the main vegetation groups (Bargain et al., 2013; Beach et al., 1997),

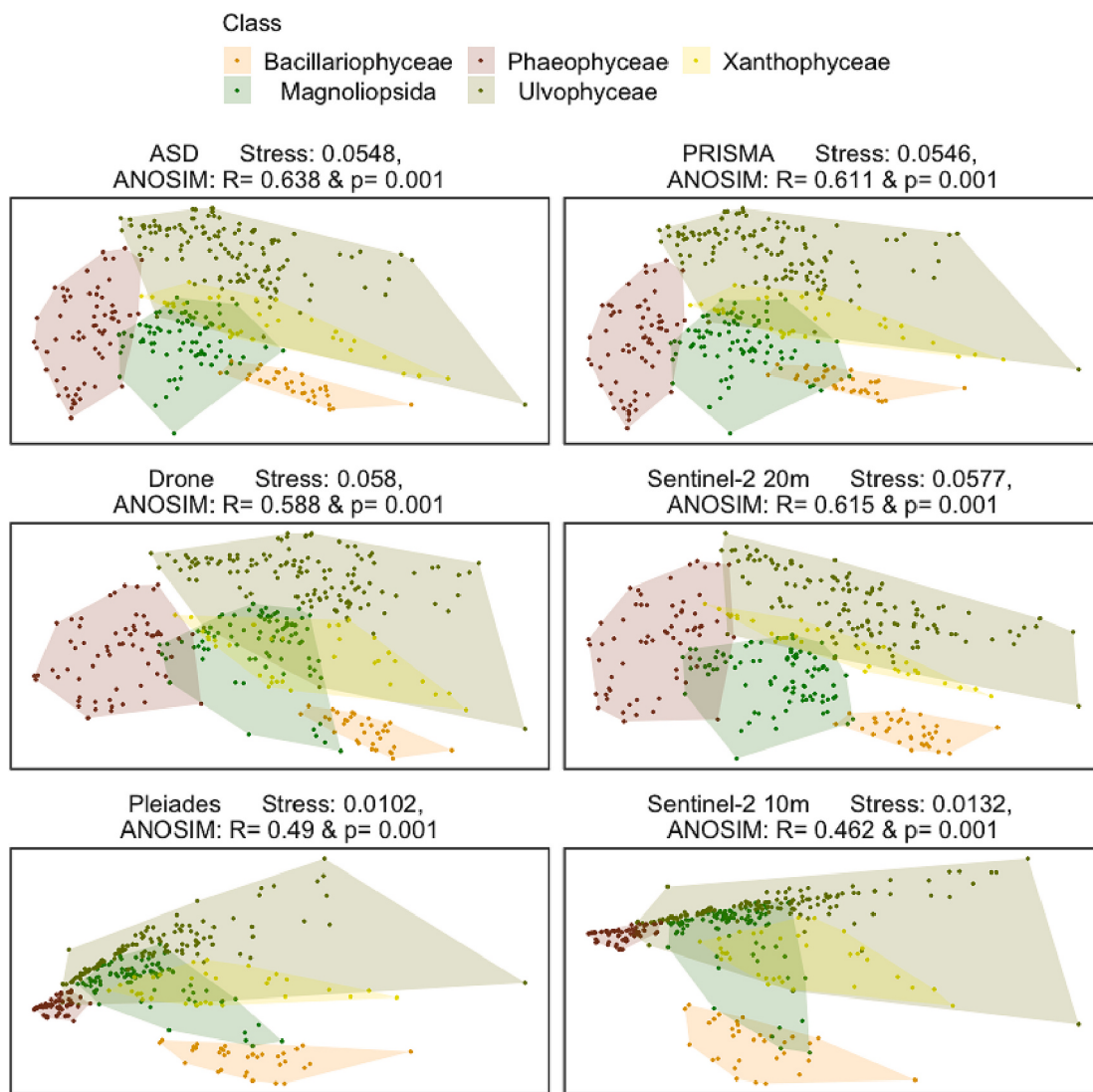


Fig. 5. nMDS ordination showing similarities between vegetation classes at different spectral resolutions (ASD, Pleiades, Sentinel-2 10, Sentinel-2 10–20 m, Drone and PRISMA). Point distances are based on cosine distance, polygons show the minimum convex hull to surround all points. Stress values show the inaccuracy of the 2 dimensional representations.

contribute to the spectral discrimination between taxonomic classes sharing the same pigment composition. Variations in the configuration of photosynthetic and accessory pigments in the 3D pigment-protein complexes within cells can also change the absorption features of taxons sharing the same pigments (Kirk, 1994), while 3D disposition of the plants as a whole can alter the magnitude of reflectance (Hedley et al., 2018). As pigment absorptions correspond to narrow spectral bands (Douay et al., 2022; Méléder et al., 2013), discriminating the different types of intertidal vegetation relies on access to these specific absorption wavelengths, which explains why the hyperspectral sensors are generally more accurate than the multispectral sensors. For the latter, the lack of relevant spectral bands and the large width of the available ones does not permit to capture the diagnostic absorption features. NIR wavelengths have long been recognised as relevant for the spectral discrimination of terrestrial plant diversity (Schmidt and Skidmore, 2003). At these wavelengths, spectral signatures are mainly a function of light scattering determined by the internal structure of leaves for angiosperms or thallus for macroalgae (Guyot, 1990). Fyfe (2003) showed that seagrass species could be separated using NIR wavelengths, with a significant change in the slopes between 700 and 900 nm. In our study, the min-max standardisation preserved the slope changes for this spectral domain while removing the difference related to biomass variations

(Bargain et al., 2012). Within the NIR, the ~722–754 nm wavelength range was identified in our work as the most discriminant for the spectral separation of the taxonomic classes of intertidal macrophytes. The better results obtained with the Drone and Sentinel-2 (20 m) bands suggest that a multispectral sensor with 10 relevant VNIR spectral bands could discriminate the main classes considered in this study. Furthermore, the wavelengths of importance for distinguishing the taxonomic classes here showed that the sensor used by Sentinel-2 could be greatly improved by the inclusion of a band at the main peaks of importance (~517–556 nm and ~722–754 nm). Both Pleiades and Sentinel-2 at 10 m miss the peak of highest importance. Furthermore, the marginally higher performance of the Pleiades sensor compared to that of the Sentinel-2 at 10 m could be linked to the overlap of two Pleiades bands over the ~517–556 nm peak, while Sentinel-2 at 10 m only has bands either side of this peak. Thus, future satellite missions aiming to provide information on global habitat cover, especially including intertidal habitats, should aim to provide sensors with spectral patterns that cover the important wavelengths shown here. Dekker et al. (2018) highlighted the utility multispectral sensors could have for monitoring a wide range of aquatic systems, recommending ~26 bands between 380 and 780 nm, specifically 684 nm to capture chlorophyl-a fluorescence. From the current analysis focusing on intertidal habitats, the most important

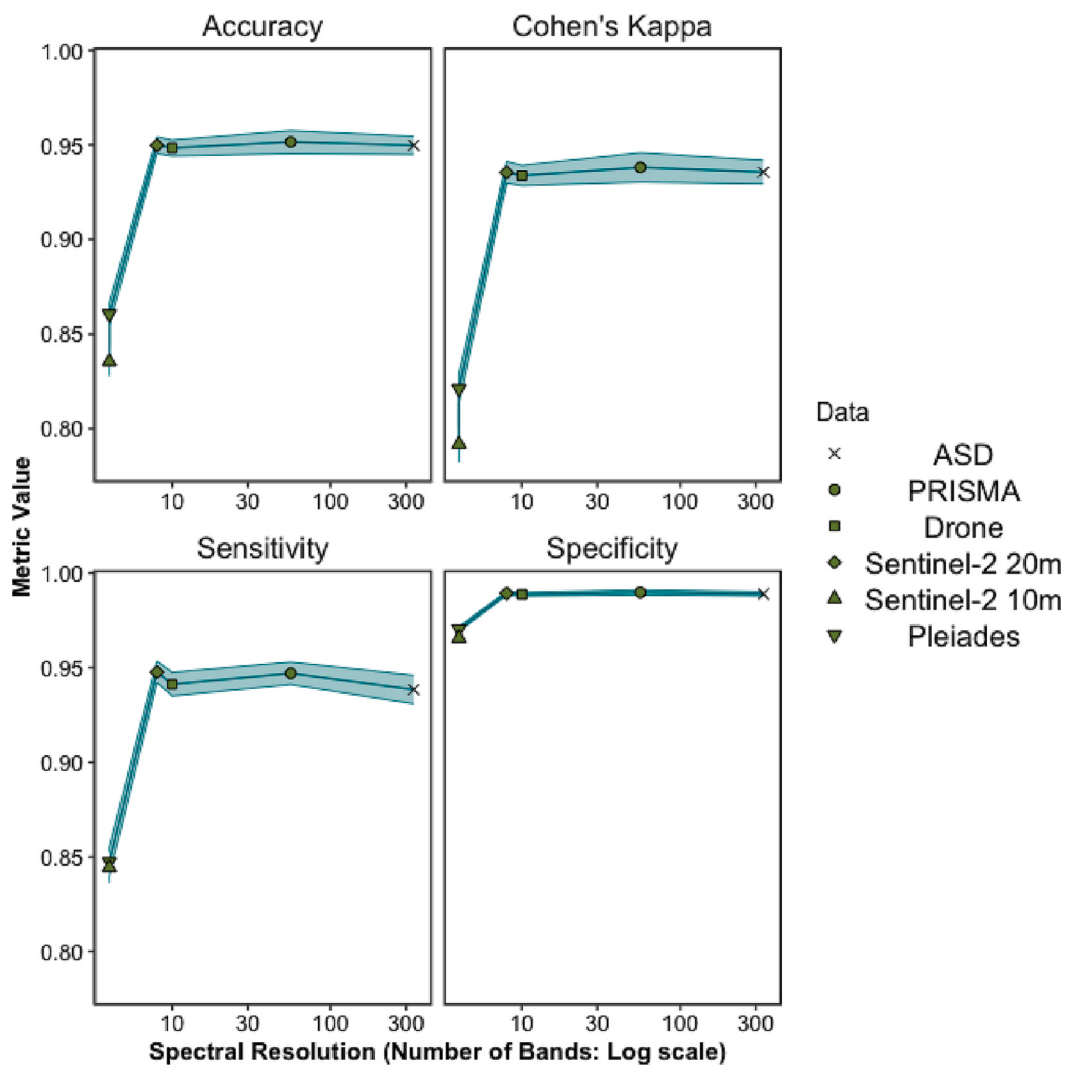


Fig. 6. Accuracy metrics (accuracy, Cohen's kappa accuracy, sensitivity and specificity) for different spectral resolutions.

Table 2

Accuracy metrics (accuracy, Cohen's kappa accuracy, sensitivity and specificity) for different spectral resolutions \pm standard error.

Sensor	Accuracy	Cohen's Kappa	Sensitivity	Specificity
Sentinel-2 10 m (4 bands)	0.835 \pm 0.00768	0.792 \pm 0.0096	0.844 \pm 0.00807	0.966 \pm 0.00162
Pleiades (4 bands)	0.861 \pm 0.00609	0.821 \pm 0.00773	0.847 \pm 0.00759	0.97 \pm 0.00126
Sentinel-2 20 m (8 bands)	0.95 \pm 0.00441	0.935 \pm 0.00577	0.948 \pm 0.00568	0.989 \pm 0.00104
Drone (10 bands)	0.948 \pm 0.00419	0.934 \pm 0.00535	0.941 \pm 0.00619	0.989 \pm 0.00094
PRISMA (56 bands)	0.951 \pm 0.0061	0.938 \pm 0.00778	0.947 \pm 0.00594	0.99 \pm 0.00129
ASD (335 bands)	0.95 \pm 0.0048	0.936 \pm 0.00624	0.938 \pm 0.00751	0.989 \pm 0.001

wavelengths to cover would be around 530 & 730 nm. The main reason for this difference with the recommendations of Dekker et al. (2018) is that their work was specifically focused on submerged vegetation and addressed a broader range of objectives. For an effective monitoring system, specific and broad objectives of the satellite will ideally dictate the spectral coverage of the sensors used.

4.3. Geographical and temporal range of applicability

The present spectral library aimed to represent a diversity of soft-bottom intertidal vegetation, with the main objective of discriminating seagrass from green macroalgae. However, it has a greater diversity of green macrophytes, making unbalanced among classes. Green macroalgae represent around 33% of the library with 121 spectra out of 366, while the yellow macroalgae only have 33 spectra. Such a difference has an impact on the statistical analysis and the discrimination results, as some species are over-represented and others underrepresented. Yet, use of Cohen's kappa, which is an accuracy metric taking into consideration this imbalance, gave minimal difference to global accuracy. This library was built with data collected on the Atlantic coasts of France, Spain and Portugal and could be improved by the addition of new species or spectra from the existing species from other sites, both across Europe and globally.

As advised by Bajjouk et al. (2019), *Z. noltei* spectral data were collected at their development peak (June to September), as it is known that these macrophytes have a seasonal pigment variation (Bargain et al., 2013). Likewise, Légaré et al. (2022) found that depending on the season, spectral reflectance from intertidal habitats can vary significantly. As such, the current spectral library should not be used outside a late spring and summer period for Western Europe, as the varying pigment content can affect the reflectance spectral shapes. Seagrass spectral analysis could also be refined by taking into account the

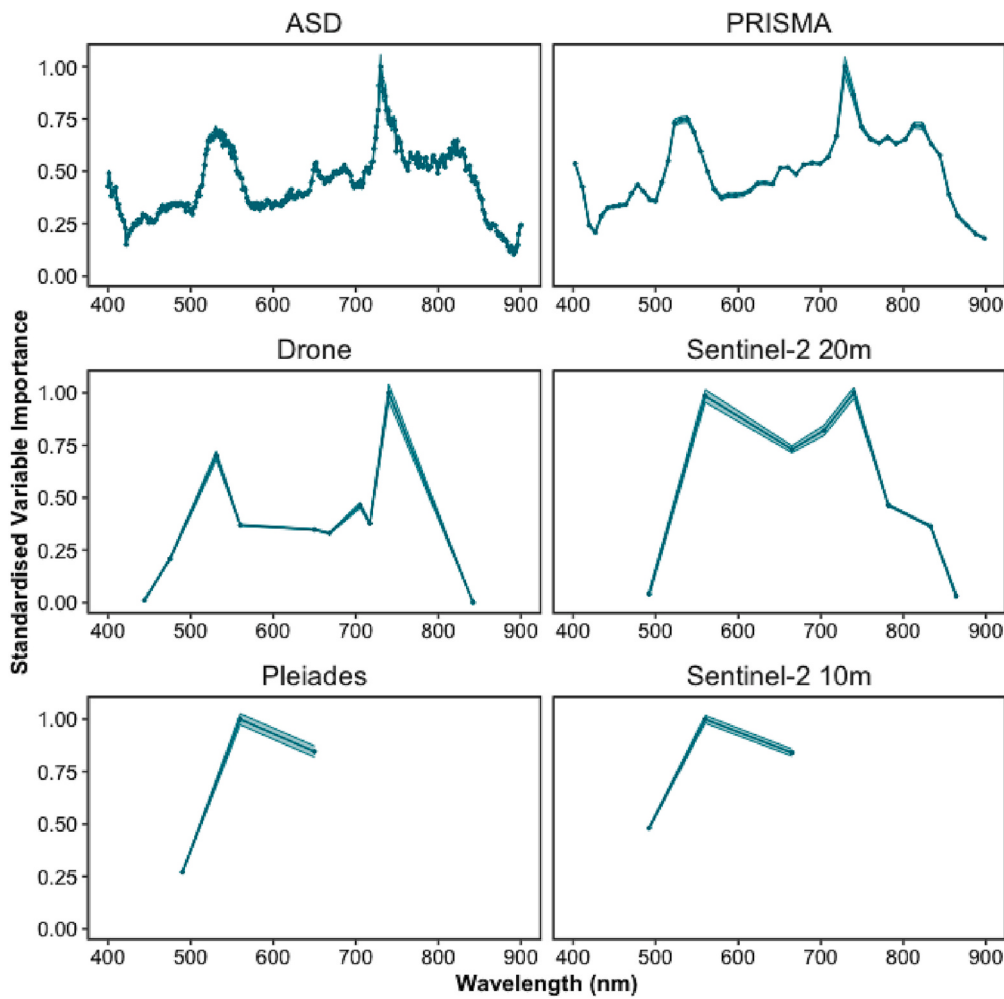


Fig. 7. The relative importance of different wavelengths for model prediction across spectral resolutions.

presence of epiphytes on their leaves, which was not done in this study. Epiphytes on seagrass leaves are known to have an impact on the shape of the reflectance spectra (Fyfe, 2003), as they are composed of diatoms and brown algae. This might explain the proximity between some seagrass and brown macroalgae spectra and the overlap between the diatoms and the seagrass (Fig. 5). The presence of epiphytes could alter the relevance of the most discriminative wavelengths between seagrass and other macroalgae. Furthermore, this library was created using 100% cover of taxonomic classes. This homogeneity is often rare at the satellite pixel scales (10–60 m), meaning future work should assess the spectral signatures of mixed intertidal vegetation to best predict extent of heterogeneous intertidal vegetation.

4.4. Implications for coastal biodiversity studies

The importance of long term monitoring of ecosystems is becoming more acknowledged, especially when monitoring human impacts that may affect Essential Biodiversity Variables (EBVs), such as important habitats, species, or the functioning of those species or habitats (Davies et al., 2022a; Davies et al., 2021; El-Hacen et al., 2020; Lengyel et al., 2008; Livore et al., 2021; Perera-Valderrama et al., 2020). This is becoming even more apparent with the acceleration of human induced climate change, which is likely to exacerbate or accelerate the effects of many other human impacts (Cramer et al., 2018; Sage, 2020). Yet, *in situ* long term monitoring of EBVs is rare (Edwards et al., 2010). This rarity is due to a range of factors, most of which are driven by financial cost, especially if multiple fieldwork campaigns per year are required to

capture seasonal variation (Condal et al., 2012). Furthermore, many human impacts can rarely be predicted *a priori*, so the ability to monitor their impact with sufficient previous data is circumstantial (Davies et al., 2022b; Sheehan et al., 2021). This prior data is imperative to properly monitor human impacts and subsequently manage the activities leading to those impacts appropriately (Edgar et al., 2004; Fox et al., 2017; Underwood, 1992). The extent, both temporally and spatially, of Earth Observation (EO) from satellite data alongside its accessibility means it has been used to study long term anthropogenic impacts (Hu et al., 2017; Lizcano-Sandoval et al., 2022; Santos et al., 2020; Zoffoli et al., 2021). Unlike *in situ* monitoring data, past EO data are easily available, meaning that the long term manifestation of novel phenomena can be assessed effectively (Mahrad et al., 2020). Here, it was shown that spectral reflectance measurements from a relatively low spectral resolution sensor (8–10 bands: e.g. sensor of Sentinel-2 at 20 m resolution) could effectively and accurately classify soft-bottom intertidal vegetative habitats. However, the importance of spectral coverage has also been highlighted; when EO is being utilised, the specific response functions of sensors need to be aligned effectively with the objectives of the analysis. These considerations, alongside the temporal and spatial scales; revisit times of satellites, and the ability for satellites sensors to effectively observe important spectral differences after atmospheric correction is applied, will dictate the most appropriate satellites to be included in a Global Ocean Observing System (GOOS) for optimal monitoring and understanding of the Essential Ocean Variables (EOVs) in coastal ecosystems studies.

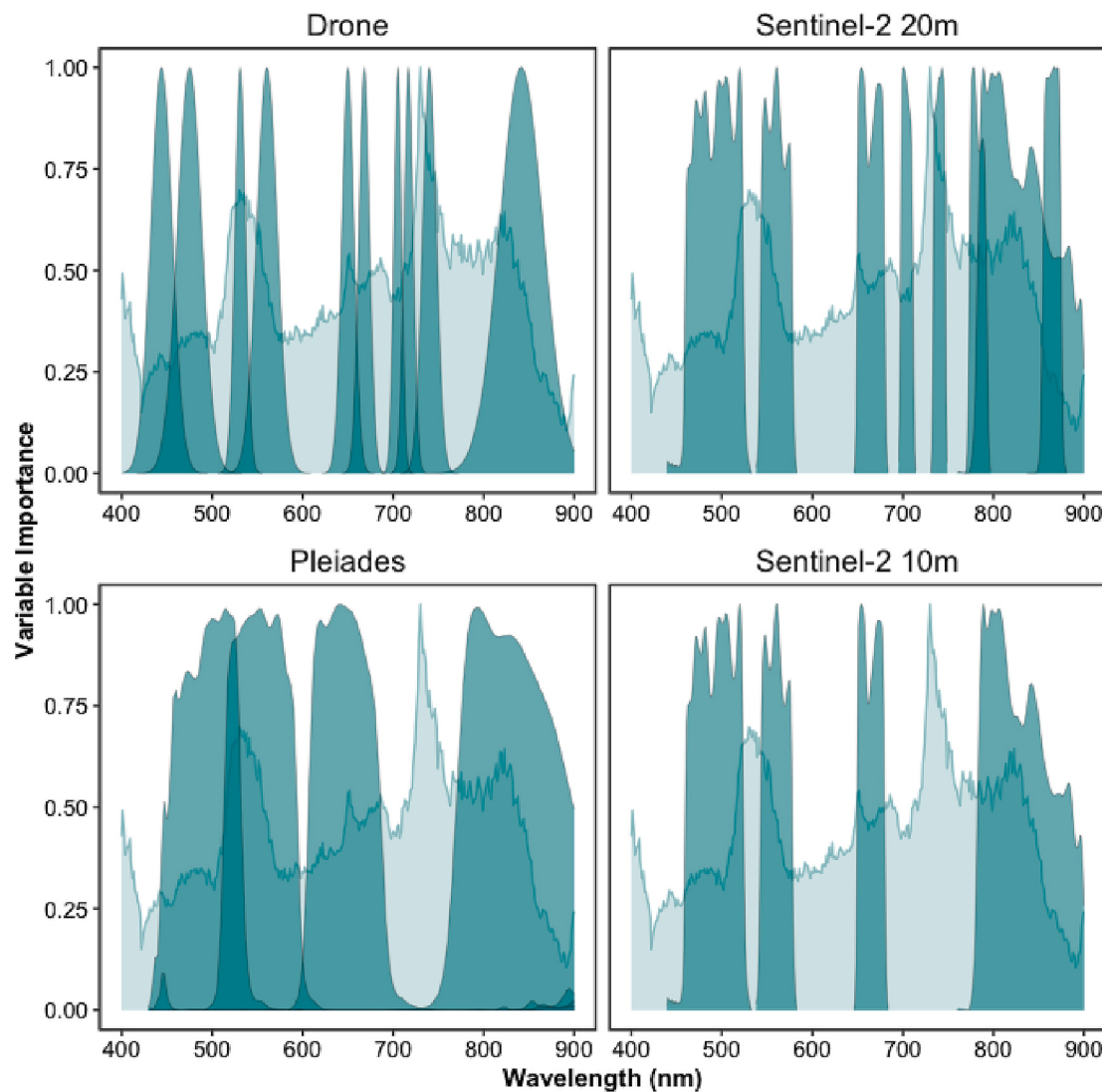


Fig. 8. The relative importance of different wavelengths for ASD model prediction across the spectral bands of the Drone, Sentinel-2 and Pleiades sensors.

4.5. Conclusions

Here, the ability to distinguish between five different vegetative intertidal habitats was assessed by analysing their spectral reflectance signatures. Around 366 spectra were compiled across the European Atlantic coast, from Southern Spain to Northern France. The spectral library was analysed at different multi- and hyperspectral resolutions with the emphasis on comparing commonly used satellite and drone sensors. This analysis not only highlighted the ability of a random forest spectral classification model to distinguish between differently pigmented habitats but also between similarly pigmented classes (green algae and seagrass). This approach could aid with ongoing efforts to accurately estimate global seagrass extent, alongside common methods such as Normalised Difference Vegetation Index (NDVI) that can provide proxies for vegetation coverage, such as monospecific intertidal seagrass meadow (Zoffoli et al., 2020). In particular, our work demonstrated the potential of discriminating intertidal seagrass from Ulvophyceae using satellite remote sensing, therefore unlocking a strong limitation for seagrass mapping in heterogeneous environments. High accuracy at distinguishing habitats was found for hyperspectral sensors as well as multispectral sensors consisting of >8 bands in the visible and near-infrared (ASD, PRISMA, Sentinel-2 at 20 m resolution and the MicaSense RedEdge MX-dual Drone sensor). As climate change alongside

other anthropogenic activities continue to impact community stability and functions, and potentially alter ecosystem services, monitoring of habitats becomes ever more important. Intertidal habitats are a vital link between terrestrial and coastal marine ecosystems, yet due to their dynamic nature and inaccessibility are difficult to assess. Therefore, the ability to monitor these ecosystems over time with high spatial and temporal resolution is important. This research provides the evidence that soft-bottom intertidal green macrophytes can be accurately classified at spectral resolutions currently available from satellite missions, assuming consistency after atmospheric correction, thus offering new perspectives for EO biodiversity studies of intertidal ecosystems. It further provides advice for the next generation of satellite missions in terms of optimal spectral resolution and important wavelengths.

Credit author statement

Bede Ffinian Rowe Davies: Conceptualisation, Methodology, Formal analysis, Investigation, Writing – original draft, Writing – review & editing, Visualisation. Pierre Gernez: Conceptualisation, Methodology, Writing – review & editing, Supervision, Project administration, Funding acquisition. Andréa Geraud: Conceptualisation, Methodology, Data Organisation and Collection, Simon Oiry: Conceptualisation, Methodology, Data Organisation and Collection, Writing – review & editing,

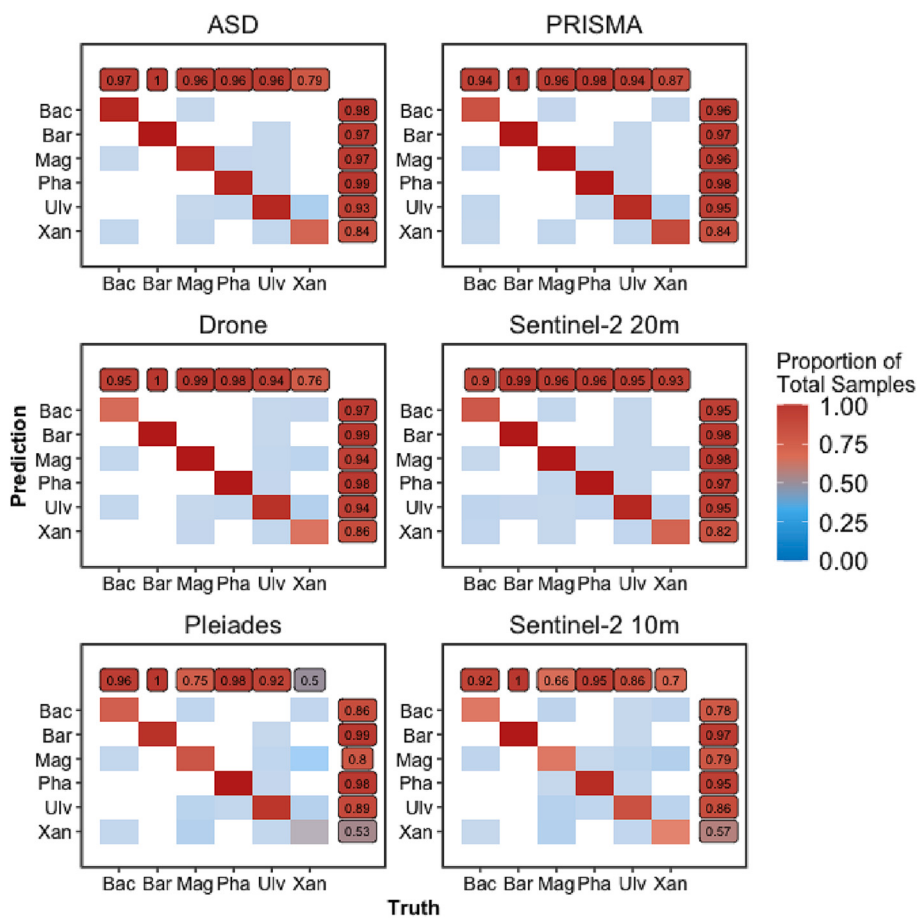


Fig. 9. Confusion matrices for different spectral resolutions. Colour of tiles show proportion of correct predictions across all 20 repetitions with no colour for 0 predictions. Classes were abbreviated Bacillariophyceae as Bac, Bare Sediments as Bar, Magnoliopsida as Mag, Phaeophyceae as Pha and Ulvophyceae as Ulv. Labels with numbers show within class sensitivity and specificity.

Table 3

Photosynthetic and carotenoid pigments present (1) or absent (0) in each taxonomic class, along with their absorption wavelength measured *in vivo* and *in vitro* with an ASD spectroradiometer and by High Performance Liquid Chromatography (HPLC) respectively. Chl b: chlorophyll b, Chl c: chlorophyll c, Fuco: fucoxanthin, Zea: zeaxanthin, Diato: diatoxanthin, Diadino: diadinoxanthin, Neo: neoxanthin.

Class	Chl b	Chl c	Fuco	Zea	Diato	Diadino	Neo	Lutein	Source
Magnoliopsida	1	0	0	1	0	0	1	1	Ralph et al., 2002
Ulvophyceae	1	0	0	1	0	0	1	1	Douay et al., 2022
Xanthophyceae	0	1	0	1	1	1	0	0	Christensen et al., 1977
Phaeophyceae	0	1	1	1	0	0	0	0	Douay et al., 2022
Bacillariophyceae	0	1	1	0	1	1	0	0	Cartaxana et al., 2016
Absorption wavelength (ASD)	650	636	550	489	496	496	—	500	Méléder et al., 2013
Absorption wavelength (HPLC)	458, 596,	442, 573,	451,	452,	453,	420, 447,	414, 437,	421, 446,	Méléder et al., 2013
	646	630	465	478	481	477	466	474	

Philippe Rosa: Conceptualisation, Methodology, Data Organisation and Collection, Writing – review & editing, Maria Laura Zoffoli: Conceptualisation, Methodology, Data Organisation and Collection, Writing – review & editing & Laurent Barillé: Conceptualisation, Methodology, Writing – review & editing, Supervision, Project administration, Funding acquisition.

Declaration of Competing Interest

The authors declare that they have no known competing financial interests or personal relationships that could have appeared to influence the work reported in this paper.

Data availability

Data will be made available on request.

Acknowledgments

This work was supported through the BiCOME (Biodiversity of the Coastal Ocean: Monitoring with Earth Observation) project funded by the European Space Agency under ‘Earth Observation Science for Society’ element of FutureEO-1 BIODIVERSITY+PRECURSORS call, contract No. 4000135756/21/I-EF.

References

- ASI, 2020. PRISMA products specification document issue 2.3 date 12/03/2020.
- Bajjouk, T., Zarati, I., Drumetz, L., Mura, M.D., 2019. 2019 10th Workshop on Hyperspectral Imaging and Signal Processing: Evolution in Remote Sensing (WHISPERS) 1–5 (Spatial characterization of marine vegetation using semisupervised hyperspectral unmixing).
- Bargain, A., Robin, M., Le Men, E., Huete, A., Barillé, L., 2012. Spectral response of the seagrass *Zostera noltii* with different sediment backgrounds. *Aquat. Bot.* 98, 45–56.
- Bargain, A., Robin, M., Méléder, V., Rosa, P., Le Menn, E., Harin, N., Barillé, L., 2013. Seasonal spectral variation of *Zostera noltii* and its influence on pigment-based vegetation indices. *J. Exp. Mar. Biol. Ecol.* 446, 86–94. <https://doi.org/10.1016/j.jembe.2013.04.012>.
- Barillé, L., Mouget, J.L., Méléder, V., Rosa, P., Jesus, B., 2011. Spectral response of benthic diatoms with different sediment backgrounds. *Remote Sens. Environ.* 115, 1034–1042. <https://doi.org/10.1016/j.rse.2010.12.008>.
- Barillé, L., Robin, M., Harin, N., Bargain, A., Launeau, P., 2010. Increase in seagrass distribution at Bourgneuf Bay (France) detected by spatial remote sensing. *Aquat. Bot.* 92, 185–194. <https://doi.org/10.1016/j.aquabot.2009.11.006>.
- Beach, K.S., Borges, H.B., Nishimura, N.J., Smith, C.M., 1997. In vivo absorbance spectra and the ecophysiology of reef macroalgae. *Coral Reefs* 16, 21–28. <https://doi.org/10.1007/s003380050055>.
- Beltrand, M., Dineen, A., Hitzether, C., Baum, B., de Cerff, C., de Vos, C., Lewis, J., Zaroufis, S., Pillay, D., 2022. Warming effects on two autogenic engineers (*Zostera capensis* and *Gracilaria gracilis*): consequences for macrofaunal assemblages and benthic heterogeneity in intertidal sandflat ecosystems. *Estuar. Coasts* 45, 247–259. <https://doi.org/10.1007/s12237-021-00949-8>.
- Brondizio, E.S., Settele, J., Diaz, S., Ngo, H.T. (Eds.), 2019. IPBES (2019), Global assessment report of the Intergovernmental Science-Policy Platform on Biodiversity and Ecosystem Services.
- Bryndum-Buchholz, A., Tittensor, D.P., Blanchard, J.L., Cheung, W.W., Coll, M., Galbraith, E.D., Jennings, S., Maury, O., Lotze, H.K., 2019. Twenty-first-century climate change impacts on marine animal biomass and ecosystem structure across ocean basins. *Glob. Chang. Biol.* 25, 459–472.
- Cao, F., Yang, Z., Ren, J., Jiang, M., Ling, W.-K., 2017. Normalization Methods Play a Role for Hyperspectral Image Classification? 2–7.
- Cardoso, P., Pardal, M., Lillebø, A., Ferreira, S., Raffaelli, D., Marques, J., 2004. Dynamic changes in seagrass assemblages under eutrophication and implications for recovery. *J. Exp. Mar. Biol. Ecol.* 302, 233–248.
- Cartaxana, Paulo, Cruz, Sónia, Gameiro, Carla, Kühl, Michael., 2016. Regulation of intertidal microphytobenthos photosynthesis over a diel emersion period is strongly affected by diatom migration patterns. *Frontiers in Microbiology* 7, 1–11.
- Casal, G., Kutser, T., Domínguez-Gómez, J.A., Sánchez-Carnero, N., Freire, J., 2013. Assessment of the hyperspectral sensor CASI-2 for macroalgal discrimination on the Ría de Vigo coast (NW Spain) using field spectroscopy and modelled spectral libraries. *Cont. Shelf Res.* 55, 129–140. <https://doi.org/10.1016/j.csr.2013.01.010>.
- Casal, G., Sánchez-Carnero, N., Domínguez-Gómez, J.A., Kutser, T., Freire, J., 2012. Assessment of AHS (Airborne hyperspectral Scanner) sensor to map macroalgal communities on the Ría de Vigo and Ría de Aldán coast (NW Spain). *Mar. Biol.* 159, 1997–2013. <https://doi.org/10.1007/s00227-012-1987-5>.
- Chao Rodríguez, Y., Domínguez Gómez, J.A., Sánchez-Carnero, N., Rodríguez-Pérez, D., 2017. A comparison of spectral macroalgae taxa separability methods using an extensive spectral library. *Algal Res.* 26, 463–473. <https://doi.org/10.1016/j.algal.2017.04.021>.
- Christensen, T., Dixon, P.S., Irvine, L.M., 1977. Seaweeds of the British Isles: *Tribophyceae* (xanthophyceae). British Museum (Natural History).
- Condal, F., Aguzzi, J., Sarda, F., Nogueras, M., Cadena, J., Costa, C., Del Rio, J., Manuel, A., 2012. Seasonal rhythm in a Mediterranean coastal fish community as monitored by a cabled observatory. *Mar. Biol.* 159, 2809–2817.
- Cramer, W., Guiot, J., Fader, M., Garrabou, J., Gattuso, J.-P., Iglesias, A., Lange, M.A., Lionello, P., Llasat, M.C., Paz, S., et al., 2018. Climate change and interconnected risks to sustainable development in the Mediterranean. *Nat. Clim. Chang.* 8, 972–980.
- Davies, B.F., Holmes, L., Bicknell, A., Attrill, M.J., Sheehan, E.V., 2022. A decade implementing ecosystem approach to fisheries management improves diversity of taxa and traits within a marine protected area in the UK. *Divers. Distrib.* 28, 173–188.
- Davies, B.F., Holmes, L., Rees, A., Attrill, M.J., Cartwright, A.Y., Sheehan, E.V., 2021. Ecosystem approach to fisheries management works—how switching from mobile to static fishing gear improves populations of fished and non-fished species inside a marine-protected area. *J. Appl. Ecol.* 58, 2463–2478.
- Davies, B.F.R., Holmes, L., Attrill, M.J., Sheehan, E.V., 2022. Ecosystem benefits of adopting a whole-site approach to MPA management. *Fish. Manag. Ecol.* 29 (6), 790–805.
- Dekker, A.G., Pinnel, N., Gege, P., Briottet, X., Peters, S., Turpie, K.R., Sterckx, S., Costa, M., Giardino, C., Brando, V.E., 2018. Feasibility study for an aquatic ecosystem earth observing system version 1.2.
- Dierssen, H.M., Chlus, A., Russell, B., 2015. Hyperspectral discrimination of floating mats of seagrass wrack and the macroalgae sargassum in coastal waters of greater Florida Bay using airborne remote sensing. *Remote Sens. Environ.* 167, 247–258. <https://doi.org/10.1016/j.rse.2015.01.027>.
- Diruit, W., Le Bris, A., Bajjouk, T., Richier, S., Helias, M., Burel, T., Lennon, M., Guyot, A., Ar Gall, E., 2022. Seaweed habitats on the shore: characterization through hyperspectral UAV imagery and field sampling. *Remote Sens.* 14, 3124.
- Douay, F., Verpoorter, C., Duong, G., Spilmont, N., Gevaert, F., 2022. New hyperspectral procedure to discriminate intertidal macroalgae. *Remote Sens.* 14, 346.
- Durou, C., Poirier, L., Amiard, J.-C., Budzinski, H., Gnassis-Barelli, M., Lemenach, K., Peluhet, L., Mouneyrac, C., Roméo, M., Amiard-Triquet, C., 2007. Biomonitoring in a clean and a multi-contaminated estuary based on biomarkers and chemical analyses in the endobenthic worm *nereis diversicolor*. *Environ. Pollut.* 148, 445–458.
- Edgar, G., Bustamante, R., Farina, J.-M., Calvopina, M., Martinez, C., Toral-Granda, M., 2004. Bias in evaluating the effects of marine protected areas: the importance of baseline data for the Galapagos marine reserve. *Environ. Conserv.* 31, 212–218.
- Edwards, M., Beaugrand, G., Hays, G.C., Koslow, J.A., Richardson, A.J., 2010. Multi-decadal oceanic ecological datasets and their application in marine policy and management. *Trends Ecol. Evol.* 25, 602–610.
- El-Hacen, E.-H.M., Cheikh, M.A.S., Bouma, T.J., Olff, H., Piersma, T., 2020. Long-term changes in seagrass and benthos at banc d'arguin, Mauritania, the premier intertidal system along the East Atlantic flyway. *Glob. Ecol. Conserv.* 24, e01364.
- Fox, H.E., Barnes, M.D., Ahmadi, G.N., Kao, G., Glew, L., Haisfield, K., Hidayat, N.I., Huffard, C.L., Katz, L., Mangubhai, S., et al., 2017. Generating actionable data for evidence-based conservation: the global center of marine biodiversity as a case study. *Biol. Conserv.* 210, 299–309.
- Fyfe, S.K., 2003. Spatial and temporal variation in spectral reflectance: are seagrass species spectrally distinct? *Limnol. Oceanogr.* 48, 464–479. https://doi.org/10.4319/lo.2003.48.1.part_2.0464.
- Gardner, R.C., Finlayson, C., 2018. Global wetland outlook: state of the world's wetlands and their services to people. Ramsar Convention Secretariat. 2020–2025.
- Garmendia, J.M., Valle, M., Borja, Á., Chust, G., Rodríguez, J.G., Franco, J., 2021. Estimated footprint of shellfishing activities in *Zostera noltii* meadows in a northern Spain estuary: lessons for management. *Estuar. Coast. Shelf Sci.* 254 <https://doi.org/10.1016/j.ecss.2021.107320>.
- Gomes, I., Peteiro, L., Bueno-Pardo, J., Albuquerque, R., Perez-Jorge, S., Oliveira, E.R., Alves, F.L., Queiroga, H., 2018. What's a picture really worth? On the use of drone aerial imagery to estimate intertidal rocky shore mussel demographic parameters. *Estuar. Coast. Shelf Sci.* 213, 185–198.
- Green, A.E., Unsworth, R.K., Chadwick, M.A., Jones, P.J., 2021. Historical analysis exposes catastrophic seagrass loss for the United Kingdom. *Front. Plant Sci.* 261.
- Greenwell, B., Boehmke, B., Gray, B., 2020. Vip: Variable importance plots.
- Guyot, G., 1990. Optical properties of vegetation canopies. Optical properties of vegetation canopies. 19–43.
- Hallik, L., Kazantsev, T., Kuusk, A., Galmés, J., Tomás, M., Niinemets, Ü., 2017. Generality of relationships between leaf pigment contents and spectral vegetation indices in mallorca (spain). *Reg. Environ. Chang.* 17, 2097–2109.
- Hedley, J.D., Mirhakak, M., Wentworth, A., Dierssen, H.M., 2018. Influence of three-dimensional coral structures on hyperspectral benthic reflectance and water-leaving reflectance. *Appl. Sci.* 8 <https://doi.org/10.3390/app8122688>.
- Hestir, E.L., Brando, V.E., Bresciani, M., Giardino, C., Matta, E., Villa, P., Dekker, A.G., 2015. Measuring freshwater aquatic ecosystems: the need for a hyperspectral global mapping satellite mission. *Remote Sens. Environ.* 167, 181–195. <https://doi.org/10.1016/j.rse.2015.05.023>.
- Hope, J.A., Coco, G., Ladewig, S.M., Thrush, S.F., 2021. The distribution and ecological effects of microplastics in an estuarine ecosystem. *Environ. Pollut.* 288, 117731 <https://doi.org/10.1016/j.envpol.2021.117731>.
- Hu, L., Hu, C., Ming-Xia, H.E., 2017. Remote estimation of biomass of *Ulva* proliferous macroalgae in the Yellow Sea. *Remote Sens. Environ.* 192, 217–227. <https://doi.org/10.1016/j.rse.2017.01.037>.
- Joyce, K.E., Belliss, S.E., Samsonov, S.V., McNeill, S.J., Glassey, P.J., 2009. A review of the status of satellite remote sensing and image processing techniques for mapping natural hazards and disasters. *Prog. Phys. Geogr.* 33, 183–207. <https://doi.org/10.1177/030913309339563>.
- Kirk, J.T., 1994. Light and Photosynthesis in Aquatic Ecosystems. Cambridge University Press.
- Kruse, A., Lefkoff, A.B., Boardman, J.W., Heidebrecht, K.B., Shapiro, A.T., Barloon, P.J., Goetz, A.F.H., 1993. In: The spectral image processing system (SIPS)-interactive visualization and analysis of imaging spectrometer data, 192, pp. 192–201. <https://doi.org/10.1063/1.44433>.
- Kuhn, M., Vaughan, D., Hvitfeldt, E., 2022. Yardstick: Tidy characterizations of model performance.
- Kuhn, M., Wickham, H., 2020. Tidymodels: a collection of packages for modeling and machine learning using tidyverse principles.
- Kutser, T., Vahtmäe, E., Martin, G., 2006. Assessing suitability of multispectral satellites for mapping benthic macroalgal cover in turbid coastal waters by means of model simulations. *Estuar. Coast. Shelf Sci.* 67, 521–529. <https://doi.org/10.1016/j.ecss.2005.12.004>.
- Légaré, B., Bélanger, S., Singh, R.K., Bernatchez, P., Cusson, M., 2022. Remote sensing of coastal vegetation phenology in a cold temperate intertidal system: implications for classification of coastal habitats. *Remote Sens.* 14, 3000.
- Lengyel, S., Kobler, A., Kutnar, L., Framstad, E., Henry, P.-Y., Babij, V., Gruber, B., Schmeller, D., Henle, K., 2008. A review and a framework for the integration of biodiversity monitoring at the habitat level. *Biodivers. Conserv.* 17, 3341–3356.
- Livore, J.P., Mendez, M.M., Miloslavich, P., Rilov, G., Bigatti, G., 2021. Biodiversity monitoring in rocky shores: challenges of devising a globally applicable and cost-effective protocol. *Ocean Coast. Manag.* 205, 105548.
- Lizcano-Sandoval, L., Anastasiou, C., Montes, E., Raulerson, G., Sherwood, E., Muller-Karger, F.E., 2022. Seagrass distribution, areal cover, and changes (1990–2021) in coastal waters off west-Central Florida, USA. *Estuar. Coast. Shelf Sci.* 108134.
- Mahrad, B.E., Newton, A., Icely, J.D., Kacimi, I., Abalansa, S., Snoussi, M., 2020. Contribution of remote sensing technologies to a holistic coastal and marine environmental management framework: a review. *Remote Sens.* 12, 2313.
- Masson-Delmotte, V., Zhai, P., Pirani, A., Connors, S.L., Péan, C., Berger, S., Caud, N., Chen, Y., Goldfarb, L., Gomis, M., 2021. Climate change 2021: The physical science

- basis. Contribution of working group I to the sixth assessment report of the intergovernmental panel on climate change 2..
- Mcilwaine, B., Casado, M.R., Leinster, P., 2019. Using 1st derivative reflectance signatures within a remote sensing framework to identify macroalgae in marine environments. *Remote Sens.* 11, 1–23. <https://doi.org/10.3390/rs11060704>.
- McKenzie, L.J., Nordlund, L.M., Jones, B.L., Cullen-Unsworth, L.C., Roelfsema, C., Unsworth, R.K.F., 2020. The global distribution of seagrass meadows. *Environ. Res. Lett.* 15.
- Méléder, V., Laviale, M., Jesus, B., Mouget, J.L., Lavaud, J., Kazemipour, F., Launeau, P., Barillé, L., 2013. In vivo estimation of pigment composition and optical absorption cross-section by spectroradiometry in four aquatic photosynthetic micro-organisms. *J. Photochem. Photobiol. B Biol.* 129, 115–124. <https://doi.org/10.1016/j.jphotobiol.2013.10.005>.
- Momota, K., Hosokawa, S., 2021. Potential impacts of marine urbanization on benthic macrofaunal diversity. *Sci. Rep.* 11, 1–12. <https://doi.org/10.1038/s41598-021-83597-z>.
- Mouritsen, K.N., Poulin, R., 2002. Parasitism, community structure and biodiversity in intertidal ecosystems. *Parasitology* 124. <https://doi.org/10.1017/s0031182002001476>.
- Muller-Karger, F.E., Hestir, E., Ade, C., Turpie, K., Roberts, D.A., Siegel, D., Miller, R.J., Humm, D., Izenberg, N., Keller, M., Morgan, F., Frouin, R., Dekker, A.G., Gardner, R., Goodman, J., Schaeffer, B., Franz, B.A., Pahlevan, N., Mannino, A.G., Concha, J.A., Ackleson, S.G., Cavanaugh, K.C., Romanou, A., Tzortziou, M., Boss, E.S., Pavlick, R., Freeman, A., Rousseaux, C.S., Dunne, J., Long, M.C., Klein, E., McKinley, G.A., Goes, J., Letelier, R., Kavanagh, M., Roffler, M., Bracher, A., Arrigo, K.R., Dierssen, H., Zhang, X., Davis, F.W., Best, B., Guralnick, R., Moisan, J., Sosik, H.M., Kudela, R., Mouw, C.B., Barnard, A.H., Palacios, S., Roesler, C., Drakou, E.G., Appeltans, W., Jetz, W., 2018. Satellite sensor requirements for monitoring essential biodiversity variables of coastal ecosystems. *Ecol. Appl.* 28, 749–760. <https://doi.org/10.1002/eaap.1682>.
- Murray, N.J., Phinn, S.R., DeWitt, M., Ferrari, R., Johnston, R., Lyons, M.B., Clinton, N., Thau, D., Fuller, R.A., 2019. The global distribution and trajectory of tidal flats. *Nature* 565, 222–225. <https://doi.org/10.1038/s41586-018-0805-8>.
- Nijland, W., Reshitnyk, L., Rubidge, E., 2019. Satellite remote sensing of canopy-forming kelp on a complex coastline: a novel procedure using the Landsat image archive. *Remote Sens. Environ.* 220, 41–50. <https://doi.org/10.1016/j.rse.2018.10.032>.
- Oiry, S., Barillé, L., 2021. Using sentinel-2 satellite imagery to develop microphytobenthos-based water quality indices in estuaries. *Ecol. Indic.* 121 <https://doi.org/10.1016/j.ecolind.2020.107184>.
- Oksanen, J., Simpson, G.L., Blanchet, F.G., Kindt, R., Legendre, P., Minchin, P.R., O'Hara, R.B., Solymos, P., Stevens, M.H.H., Sozees, E., Wagner, H., Barbour, M., Bedward, M., Bolker, B., Borchard, D., Carvalho, G., Chirico, M., De Caceres, M., Durand, S., Evangelista, H.B.A., FitzJohn, R., Friendly, M., Furneaux, B., Hannigan, G., Hill, M.O., Lahti, L., McGlinn, D., Ouellette, M.-H., Ribeiro Cunha, E., Smith, T., Stier, A., Ter Braak, C.J.F., Weedon, J., 2022. Vegan: Community ecology package.
- Olmedo-Masat, O.M., Paula Raffo, M., Rodríguez-Pérez, D., Arijón, M., Sánchez-Carnero, N., 2020. How far can we classify macroalgae remotely? An example using a new spectral library of species from the south West Atlantic (argentine patagonia). *Remote Sens.* 12, 1–33. <https://doi.org/10.3390/rs12233870>.
- Papanathanasopoulou, E., Simis, S.G.H., Alikas, K., Ansper, A., Anttila, S., Jenni, A., Barillé, A.-L., Barillé, L., Brando, V., Bresciani, M., Buñas, M., Gernez, P., Giardino, C., Harin, N., Hommersom, A., Kangro, K., Kaupilla, P., Koponen, S., Laanen, M., Neil, C., Papadakis, D., Peters, S., Poikane, S., Kathrin Poser, K., Pires, M. D., Riddick, C., Spyroskos, E., Tyler, A., Vaiciūtė, D., Warren, M., Zoffoli, M.L., 2019. Satellite-assisted monitoring of water quality to support the implementation of the water framework directive. EOMORES white paper 28. <https://doi.org/10.5281/zenodo.3463051>.
- Parliament, E., Council E., 2008. Directive 2008/56/ce du parlement européen et du conseil du 17 juin 2008 établissant un cadre d'action communautaire dans le domaine de la politique pour le milieu marin (directive-cadre stratégie pour le milieu marin)[en ligne]Journal Officiel de l'Union Européenne. Récupéré de. <http://eur-lex.europa.eu/legal-content/FR/TXT/PDF>.
- Parliament, E., Council, E., 2001. Directive 2000/60/CE du parlement européen et du conseil du 23 octobre 2000 établissant un cadre pour une politique communautaire dans le domaine de l'eau. Journal officiel, n L 327, 0001–0073.
- Pereira, H.M., Ferrier, S., Walters, M., Geller, G.N., Jongman, R.H.G., Scholes, R.J., Bruford, M.W., Brummit, N., Butchart, S.H.M., Cardoso, A.C., Coops, N.C., Dulloo, E., Faith, D.P., Freyhof, J., Gregory, R.D., Heip, C., Höft, R., Hurtt, G., Jetz, W., Karp, D.S., McGeoch, M.A., Obura, D., Onoda, Y., Pettorelli, N., Revers, B., Sayre, R., Scharlemann, J.P.W., Stuart, S.N., Turak, E., Walpole, M., Wegmann, M., 2013. Essential biodiversity variables. *Science* 339, 277–278.
- Perera-Valderrama, S., Cerdeira-Estrada, S., Martell-Dubois, R., Rosique-de la Cruz, L., Caballero-Aragón, H., Valdez-Chavarín, J., López-Perea, J., Ressl, R., 2020. A new long-term marine biodiversity monitoring program for the knowledge and management in marine protected areas of the Mexican caribbean. *Sustainability* 12, 7814.
- Phinn, S.R., Kovacs, E.M., Roelfsema, C.M., Canto, R.F., Collier, C.J., McKenzie, L., 2018. Assessing the potential for satellite image monitoring of seagrass thermal dynamics: for inter-and shallow sub-tidal seagrasses in the inshore great barrier reef world heritage area, Australia. *Int. J. Digital Earth* 11, 803–824.
- R Core Team, 2022. R: A Language and Environment for Statistical Computing. R Foundation for Statistical Computing, Vienna, Austria.
- Ralph, P.J., Polk, S.M., Moore, K.A., Orth, R.J., Smith, W.O., 2002. Operation of the xanthophyll cycle in the seagrass *Zostera marina* in response to variable irradiance. *J. Exp. Mar. Biol. Ecol.* 271, 189–207. [https://doi.org/10.1016/S0022-0981\(02\)00047-3](https://doi.org/10.1016/S0022-0981(02)00047-3).
- Reddin, C.J., Decottignies, P., Bacouillard, L., Barillé, L., Dubois, S.F., Echappé, C., Gernez, P., Jesus, B., Méléder, V., Nátscher, P.S., et al., 2022. Extensive spatial impacts of oyster reefs on an intertidal mudflat community via predator facilitation. *Commun. Biol.* 5, 1–11.
- Roca, M., Dunbar, M.B., Román, A., Caballero, I., Zoffoli, M.L., Gernez, P., Navarro, G., 2022. Monitoring the marine invasive alien species *rugulopteryx okamurae* using unmanned aerial vehicles and satellites. *Frontiers in marine*. Science 9.
- Sage, R.F., 2020. Global change biology: a primer. *Glob. Chang. Biol.* 26, 3–30.
- Santos, R.O., Varona, G., Avila, C.L., Lirman, D., Collado-Vides, L., 2020. Implications of macroalgae blooms to the spatial structure of seagrass seascapes: The case of the *anadyomene* spp. (*chlorophyta*) bloom in biscayne bay, florida. *Marine pollution bulletin* 150, 110742.
- Schiel, D.R., Gerrity, S., Orchard, S., Alestra, T., Dunmore, R.A., Falconer, T., Thomsen, M.S., Tait, L.W., 2021. Cataclysmic disturbances to an intertidal ecosystem: loss of ecological infrastructure slows recovery of biogenic habitats and diversity. *Front. Ecol. Evol.* 9 <https://doi.org/10.3389/fevo.2021.767548>.
- Schmidt, K., Skidmore, A., 2003. Spectral discrimination of vegetation types in a coastal wetland. *Remote Sens. Environ.* 85, 92–108.
- Sedano, F., Pavón-Paneque, A., Navarro-Barranco, C., Guerra-García, J.M., Digenis, M., Sempre-Valverde, J., Espinosa, F., 2021. Coastal armouring affects intertidal biodiversity across the Alboran Sea (Western Mediterranean Sea). *Mar. Environ. Res.* 171 <https://doi.org/10.1016/j.marenres.2021.105475>.
- Sheehan, E., Holmes, L., Davies, B., Cartwright, A., Rees, A., Attrill, M., 2021. Rewilding of protected areas enhances resilience of marine ecosystems to extreme climatic events. *Front. Marine Sci.* 8.
- Silge, J., Chow, F., Kuhn, M., Wickham, H., 2022. Rsample: General resampling infrastructure.
- Thorhaug, A., Richardson, A., Berlyn, G., 2007. Spectral reflectance of the seagrasses: *Thalassia testudinum*, *halodule wrightii*, *syringodium filiforme* and five marine algae. *Int. J. Remote Sens.* 28, 1487–1501.
- Underwood, A., 1992. Beyond BACI: the detection of environmental impacts on populations in the real, but variable, world. *J. Exp. Mar. Biol. Ecol.* 161, 145–178.
- Unsworth, R.K., Cullen-Unsworth, L.C., Jones, B.L., Lilley, R.J., 2022. The planetary role of seagrass conservation. *Science* 377, 609–613.
- Unsworth, R.K.F., McKenzie, L.J., Collier, C.J., Cullen-Unsworth, L.C., Duarte, C.M., Eklof, J.S., Jarvis, J.C., Jones, B.L., Nordlund, L.M., 2019a. Global challenges for seagrass conservation. *Ambio* 48, 801–815. <https://doi.org/10.1007/s13280-018-1115-y>.
- Unsworth, R.K.F., Nordlund, L.M., Cullen-Unsworth, L.C., 2019b. Seagrass meadows support global fisheries production. *Conserv. Lett.* 12, 1–8. <https://doi.org/10.1111/conl.12566>.
- Ustin, S.L., Jacquemoud, S., 2020. How the optical properties of leaves modify the absorption and scattering of energy and enhance leaf functionality. In: *Remote Sens. Plant Biodivers.* Springer, Cham, pp. 349–384.
- Ustin, S.L., Roberts, D.A., Gamon, J.A., Asner, G.P., Green, R.O., 2004. Using imaging spectroscopy to study ecosystem processes and properties. *Bioscience* 54, 523–534. [https://doi.org/10.1641/0006-3568\(2004\)054\[0523:USTSEJ\]2.0.CO;2](https://doi.org/10.1641/0006-3568(2004)054[0523:USTSEJ]2.0.CO;2).
- Van Der Maarel, E., 2003. Some remarks on the functions of European coastal ecosystems. *Phytocoenologia* 33, 187–202. <https://doi.org/10.1127/0340-269X/2003/0033-0187>.
- Veetil, B.K., Ward, R.D., Lima, M.D.A.C., Stankovic, M., Hoai, P.N., Quang, N.X., 2020. Opportunities for seagrass research derived from remote sensing: a review of current methods. *Ecol. Indic.* 117, 106560.
- Wright, M.N., Wager, S., Probst, P., 2022. Ranger: A fast implementation of random forests.
- Xue, J., Su, B., 2017. Significant remote sensing vegetation indices: a review of developments and applications. *J. Sens.* 2017 <https://doi.org/10.1155/2017/1353691>.
- Zoffoli, M.L., Gernez, P., Godet, L., Peters, S., Oiry, S., Barillé, L., 2021. Decadal increase in the ecological status of a North-Atlantic intertidal seagrass meadow observed with multi-mission satellite time-series. *Ecol. Indic.* 130 <https://doi.org/10.1016/j.ecolind.2021.108033>.
- Zoffoli, M.L., Gernez, P., Oiry, S., Godet, L., Dalloyau, S., Davies, B.F.R., Barillé, L., 2022. Remote sensing in seagrass ecology: coupled dynamics between migratory herbivorous birds and intertidal meadows observed by satellite during four decades. *Remote Sens. Ecol. Conserv.*
- Zoffoli, M.L., Gernez, P., Rosa, P., Le Bris, A., Brando, V.E., Barillé, A.L., Harin, N., Peters, S., Poser, K., Spaias, L., Peralta, G., Barillé, L., 2020. Sentinel-2 remote sensing of *zostera noltei*-dominated intertidal seagrass meadows. *Remote Sens. Environ.* 251, 112020 <https://doi.org/10.1016/j.rse.2020.112020>.